

Evaluation of E Layer Dominated Ionosphere Events Using COSMIC/FORMOSAT-3 and CHAMP Ionospheric Radio Occultation Data

Sumon Kamal ^{1,2,*}, Norbert Jakowski ¹, Mohammed M. Hoque ¹ and Jens Wickert ^{2,3}

¹ German Aerospace Center (DLR), Institute of Solar-Terrestrial Physics, Neustrelitz, Germany

² Technical University of Berlin, Berlin, Germany

³ GFZ German Research Centre for Geosciences, Potsdam, Germany

Reference: *Remote Sensing*, 2020, 12(2), doi: 10.3390/rs12020333

*Sumon.Kamal@dlr.de



The E Layer Dominated Ionosphere

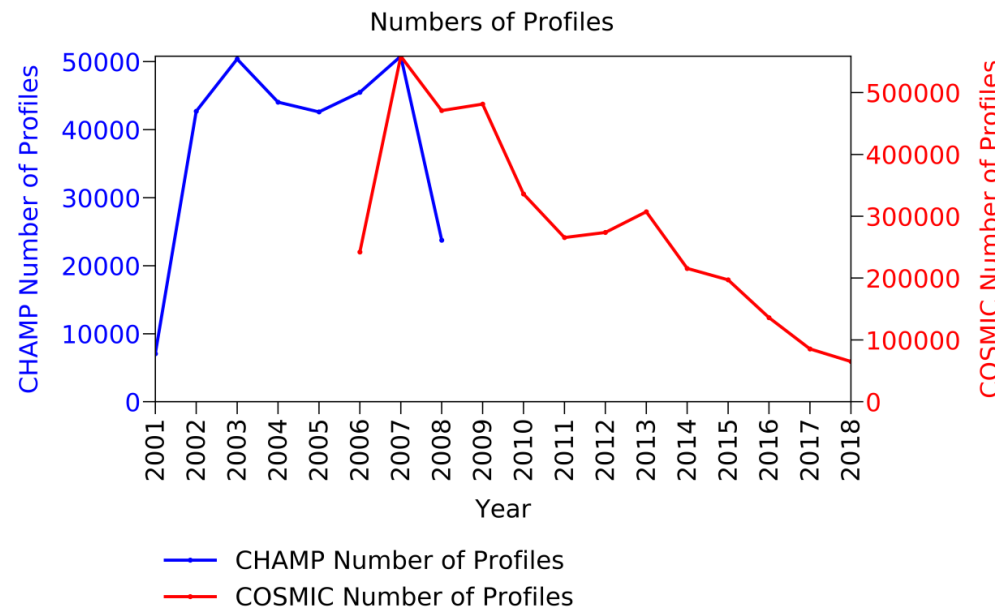
- At certain geographic locations, especially in the polar regions, the ionization of the ionospheric E layer can dominate over that of the F2 layer, which is called “E Layer Dominated Ionosphere” (ELDI).
- Electron density profiles related to ELDI show their maximum ionization at E layer heights between 80 and 150 km above the surface of the Earth.
- ELDI mainly occurs in the high latitude polar regions and is caused by particle precipitation from the magnetosphere.
- ELDI can influence radio wave propagation and thus has an effect on radio communication. It can disturb applications at high latitudes such as transpolar air traffic communication.

Investigation of ELDI occurrences

- We investigated the characteristics of ELDI occurrences at high latitudes, focusing on the following factors of influence:
 - Spatial distribution of ELDI events
 - Temporal variation of ELDI events
 - Diurnal variation
 - Seasonal variation
 - Solar cycle dependent variation
 - Geomagnetic storm dependence of ELDI events
 - Temporal variation
 - Latitudinal variation

Database

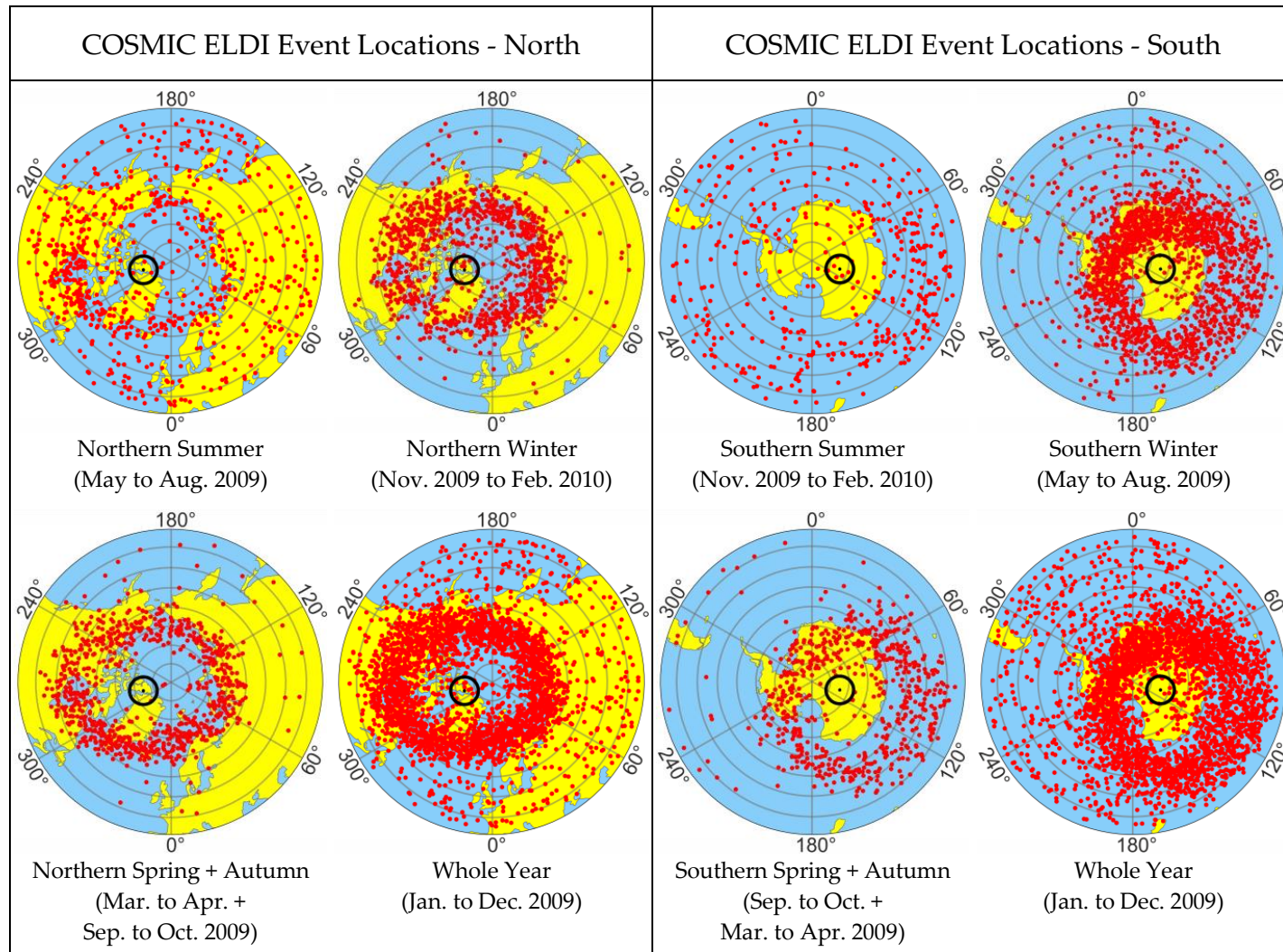
- Our database consisted of vertical electron density profiles retrieved from Ionospheric Radio Occultation observations from two different satellite missions:
 - COSMIC (Constellation Observing System for Meteorology, Ionosphere, and Climate/Formosa Satellite Mission 3) with approx. 3,635,000 profiles covering the years from 2006 to 2018
 - CHAMP (Challenging Minisatellite Payload) with approx. 307,000 profiles covering the years from 2001 to 2008



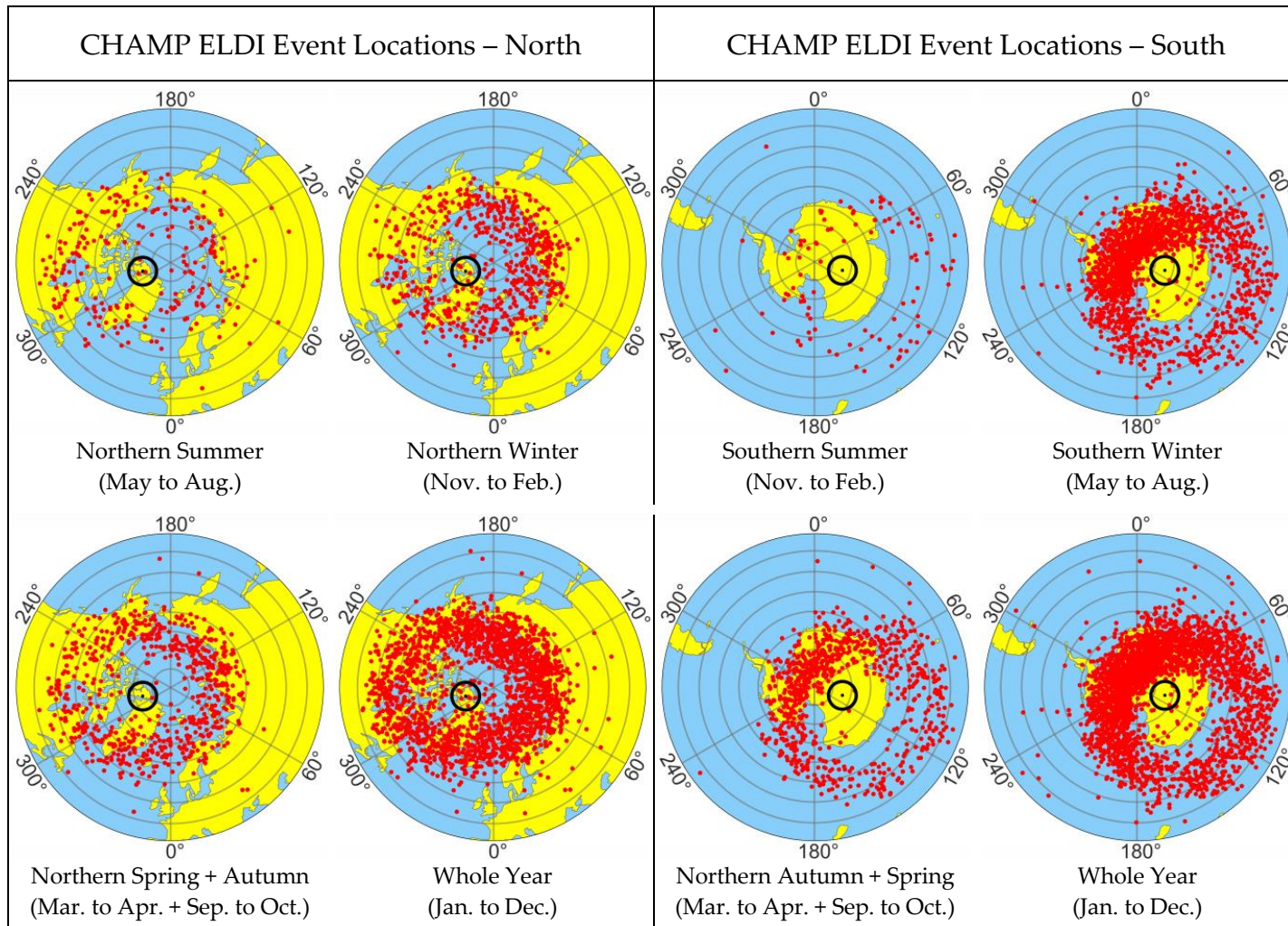
Spatial distribution of ELDI events

- Investigation:
 - Spatial distribution of ELDI events for the northern and southern high latitude regions (45° to 90°)
 - Evaluation of COSMIC electron density profiles for the year 2009 and for a superposition of CHAMP electron density profiles for the years 2001 to 2008 respectively
- Observation:
 - ELDI events (red dots) concentrate along ellipses. These are located around the geomagnetic poles (black circles)
 - Few ELDI events occur in local summer, more in spring and autumn and most in winter seasons

Spatial distribution of ELDI events - COSMIC



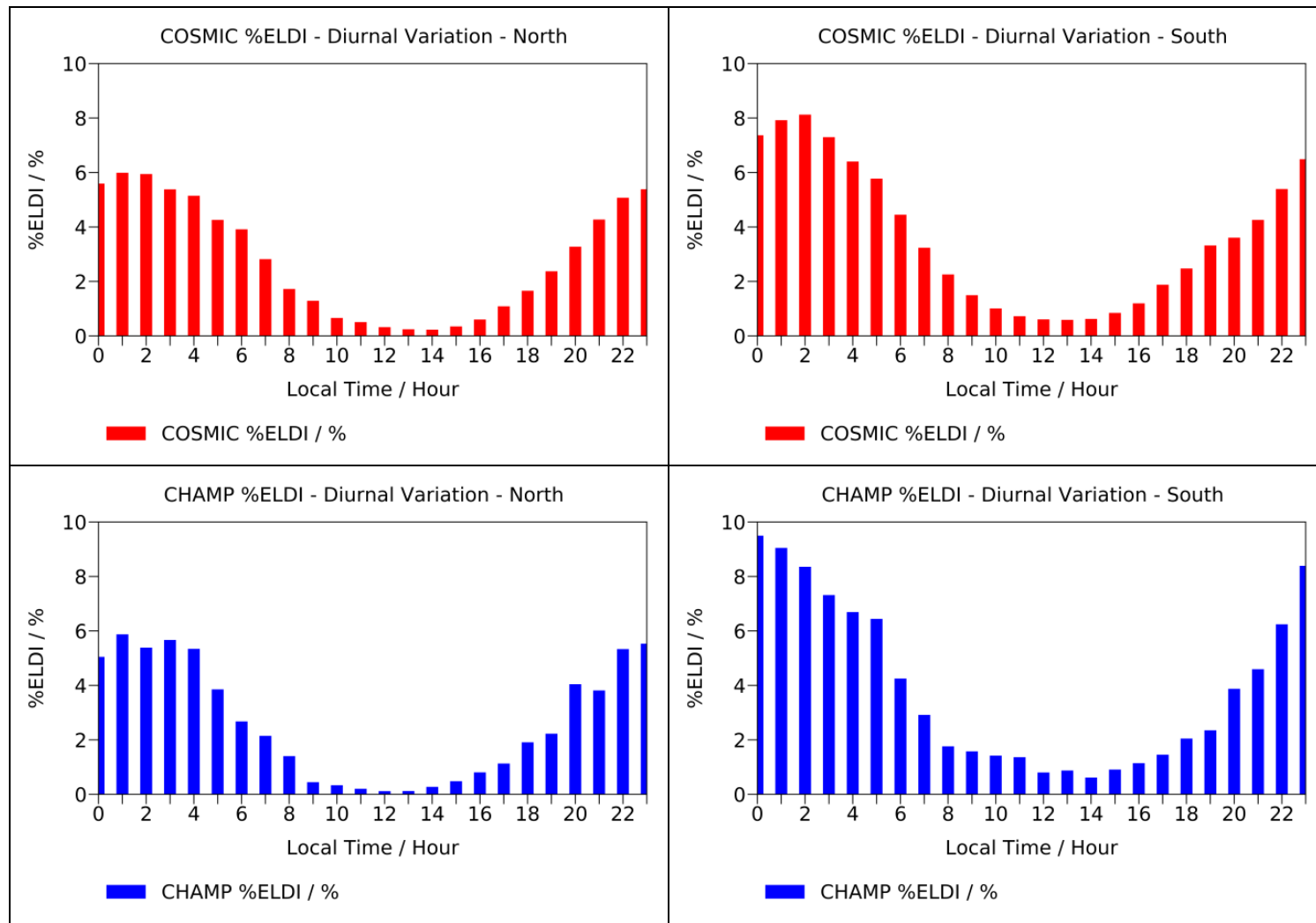
Spatial distribution of ELDI events - CHAMP



Diurnal variation of ELDI

- Investigation:
 - Diurnal variation of %ELDI (percentage of ELDI profiles compared to total number of profiles) for northern and southern high latitude regions
 - Evaluation of electron density profiles for a superposition of all years of the COSMIC data set or the CHAMP data set respectively
- Observation:
 - %ELDI reaches maximum around local night and minimum around local noon
 - Sinusoidal trend, especially for COSMIC
 - Low solar zenith angle around noon causes increased photoionization of the sunlit ionosphere
 - => F2 layer exceeds E layer ionization => few ELDI events during the day
 - Absent photoionization and increased particle precipitation on the night side
 - => E layer exceeds F2 layer ionization => many ELDI events during the night

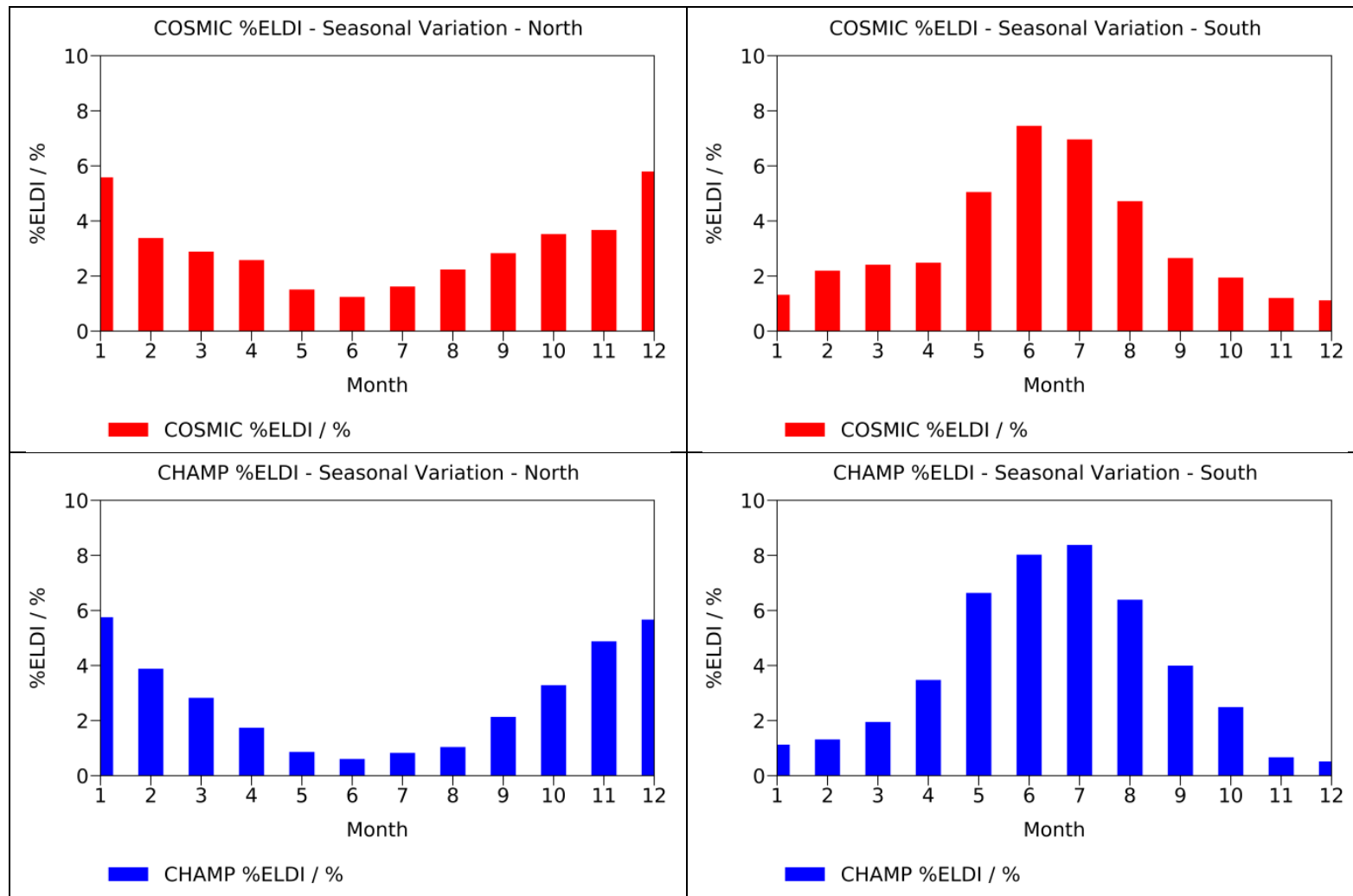
Diurnal variation of ELDI



Seasonal variation of ELDI

- Investigation:
 - Seasonal variation of %ELDI for northern and southern high latitude regions
 - Evaluation of electron density profiles for a superposition of all years of the COSMIC data set or the CHAMP data set respectively
- Observation:
 - %ELDI reaches maximum in local winter and minimum in local summer
 - Large solar zenith angle in winter causes a reduced photoionization of the F2 layer while at the same time the long nights result in an easier F2 layer degradation due to recombination processes
=> lower average F2 layer ionization increases likelihood for ELDI occurrence

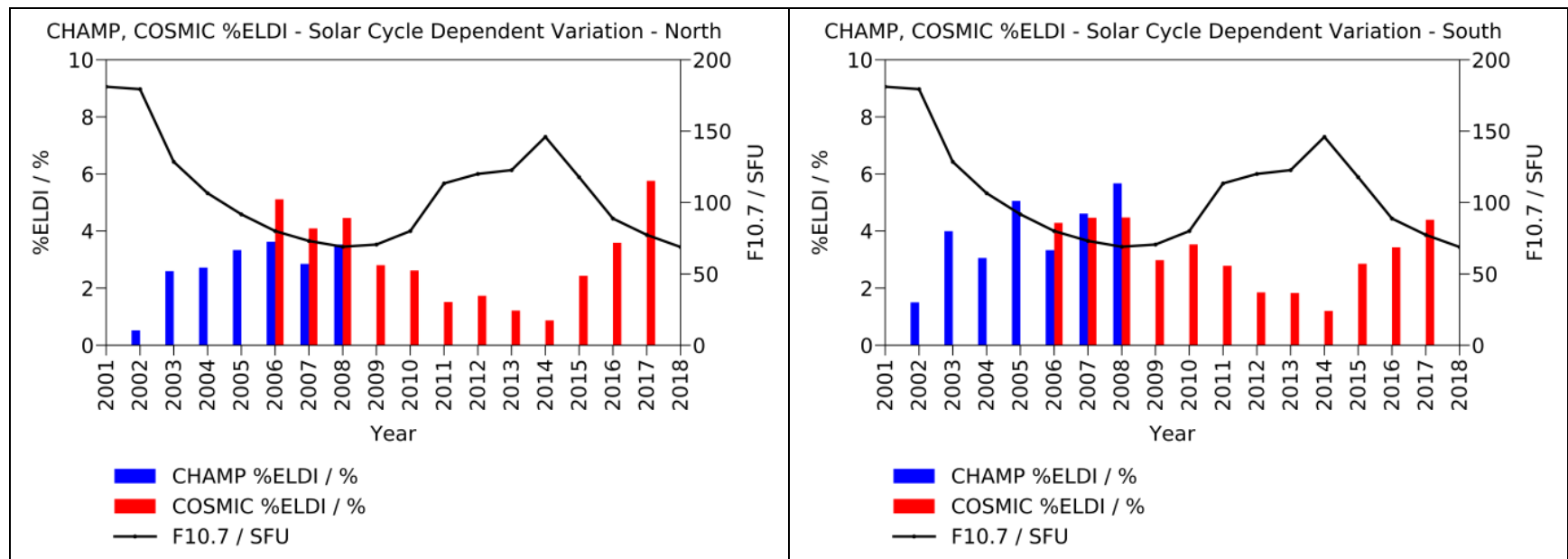
Seasonal variation of ELDI



Solar cycle dependent variation of ELDI

- Investigation:
 - Annual variation of %ELDI for northern and southern high latitude regions depending on 11 year solar cycle
 - Observation of F10.7 solar radio flux as measure for solar activity
 - Evaluation of electron density profiles for combined CHAMP and COSMIC datasets for the years 2001 to 2018, covering a full solar cycle
- Observation:
 - Low %ELDI at high solar activity level and vice versa
 - High solar activity causes increased amount of EUV radiation and therefore stronger photoionization of the F2 layer
 - => F2 layer exceeds E layer ionization resulting in less ELDI events

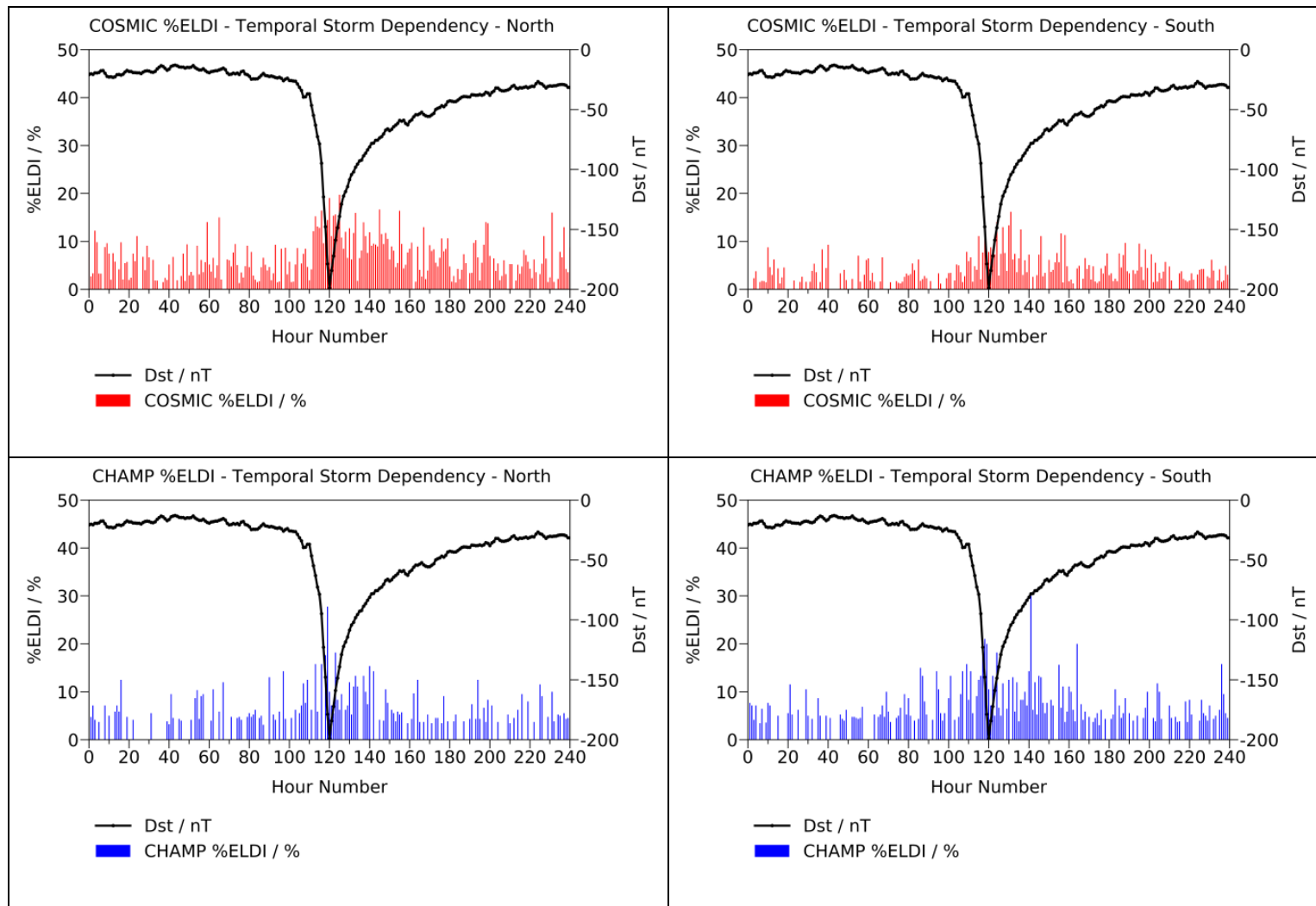
Solar cycle dependent variation of ELDI



Geomagnetic storms – Temporal variation of ELDI

- Investigation:
 - Temporal variation of %ELDI depending on occurrence of geomagnetic storms
 - Observation of Dst as measure for geomagnetic activity
 - Evaluation of 27 geomagnetic storms from the period 2001 to 2016
 - Epoch analysis for the superposition of 10-day wide windows, each one centered on one of the storms peaks
 - Separate evaluation for COSMIC and CHAMP
- Observation:
 - Storm onset phase shows sudden drop in Dst and increase of %ELDI while recovery phase shows slow increase of Dst and decrease of %ELDI
 - Geomagnetic storms are accompanied by an increased flow of solar charged particles entering the magnetosphere and precipitating into the ionosphere
=> higher average E layer ionization increases likelihood for ELDI occurrence

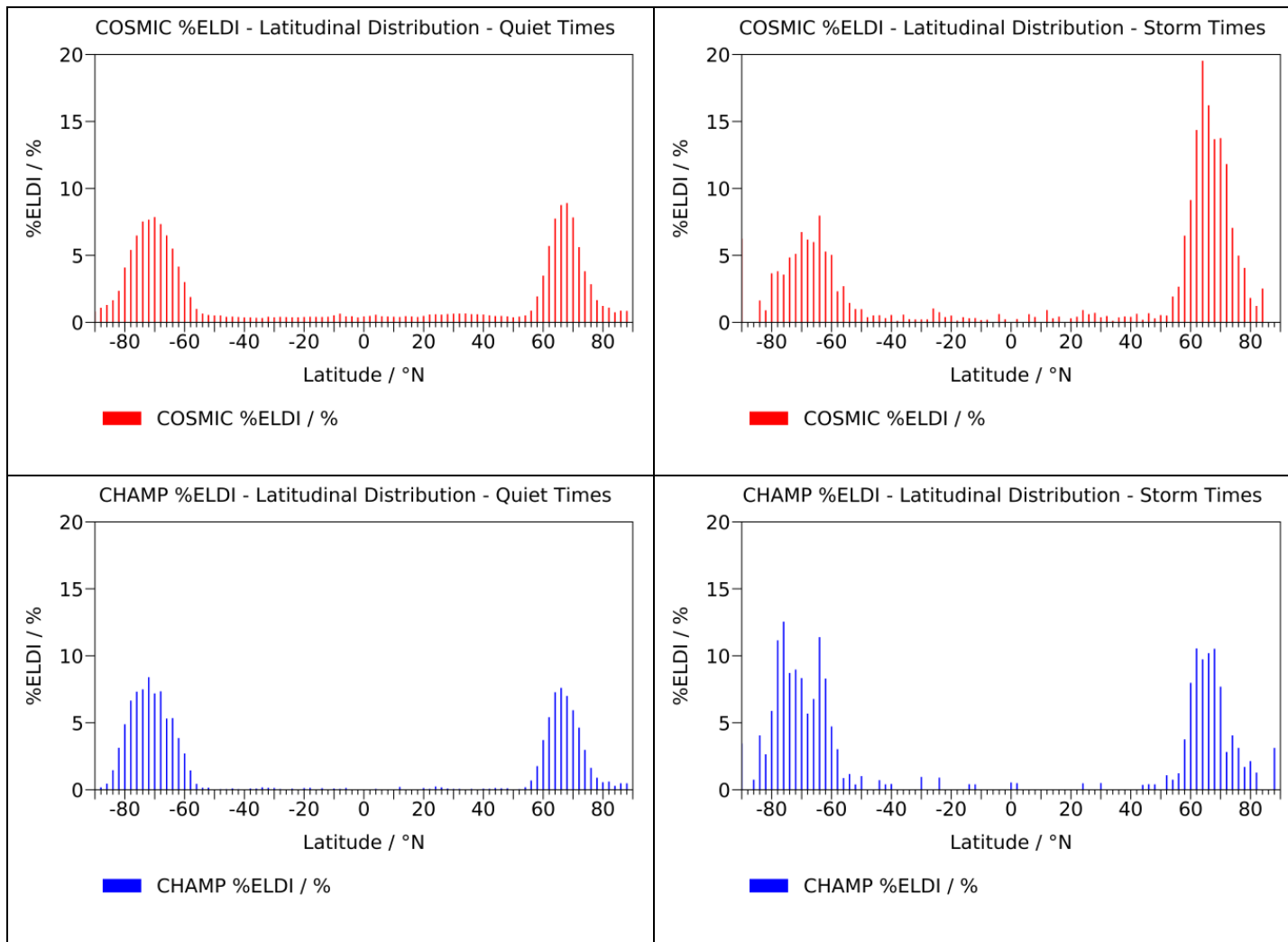
Geomagnetic storms – Temporal variation of ELDI



Geomagnetic storms – Latitudinal variation of ELDI

- Investigation:
 - Latitudinal variation of %ELDI depending on occurrence of geomagnetic storms
 - Observation of Dst as measure for geomagnetic activity
 - Analysis for quiet times and storm times (same 27 storms as in previous analysis)
 - Computation of Mean %ELDI for northern and southern hemispheres to get %ELDI peak magnitudes (“N %ELDI Mean”, “S %ELDI Mean”)
 - Computation of Mean and Root Mean Square of all latitudes weighted by %ELDI for both hemispheres to get peak positions (“N Lat Mean”, “S Lat Mean”, “N Lat RMS”, “S Lat RMS”) and computation of the distance between northern and southern Mean and RMS (“Lat Mean Dist”, “Lat RMS Dist”)
 - Separate evaluation for COSMIC and CHAMP
- Observation:
 - %ELDI peaks are higher during storm times than during quiet times
 - Peaks are located at auroral latitudes
 - Smaller distance between peaks (“Lat Mean Dist”, “Lat RMS Dist”) resulting from a shift of these to lower latitudes during storms
 - => Equatorward motion of auroral zone in case of storms

Geomagnetic storms – Latitudinal variation of ELDI



Geomagnetic storms – Latitudinal variation of ELDI

Mission	Condition	N %ELDI Mean	S %ELDI Mean	N Lat Mean	S Lat Mean	Lat Mean Dist	N Lat RMS	S Lat RMS	Lat RMS Dist
COSMIC	Quiet times	2.90	3.40	68.74°	-69.64°	138.38°	69.15°	70.12°	139.27°
	Storm times	6.35	3.64	67.80°	-68.38°	136.18°	68.13°	69.09°	137.22°
CHAMP	Quiet times	2.29	3.37	68.33°	-70.40°	138.73°	68.61°	70.73°	139.34°
	Storm times	4.15	5.49	67.87°	-70.19°	138.06°	68.31°	70.67°	138.98°

Conclusions

- We analyzed the spatiotemporal distribution of ELDI events for both hemispheres and various factors of influence on the basis of a large database that covers almost 18 years of IRO observations from the COSMIC and CHAMP missions.
- The results obtained for both satellite missions and both hemispheres are similar.
- These results are:
 - For both hemispheres, ELDI events follow an elliptical distribution in the auroral zones, which are located around the geomagnetic poles.
 - The number of ELDI events increases at nighttime and during the winter months.
 - For low solar activity the number of ELDI events increases, for high solar activity it decreases.
 - During geomagnetic storms the number of ELDI events increases while at the same time their auroral distribution moves towards the equator.
- Further investigations regarding the shape of the elliptical ELDI event distributions are planned.

References

- Hajj, G.A.; Romans, L.J. Ionospheric electron density profiles obtained with the Global Positioning System: Results from the GPS/MET experiment. *Radio Sci.* 1998, 33, 175–190, doi:10.1029/97RS03183.
- Schreiner, W.S.; Sokolovskiy, S.V.; Rocken, C.; Hunt, D.C. Analysis and validation of GPS/MET radio occultation data in the ionosphere. *Radio Sci.* 1999, 34, 949–966, doi:10.1029/1999RS900034.
- Jakowski, N.; Wehrenpfennig, A.; Heise, S.; Reigber, C.; Lühr, H.; Grunwaldt, L.; Meehan, T.K. GPS radio occultation measurements of the ionosphere from CHAMP: Early results. *Geophys. Res. Lett.* 2002, 29, 95-1–95-4, doi:10.1029/2001GL014364.
- Mayer, C.; Jakowski, N. Enhanced E-layer ionization in the auroral zones observed by radio occultation measurements onboard CHAMP and Formosat-3/COSMIC. *Ann. Geophys.* 2009, 27, 1207–1212, doi:10.5194/angeo-27-1207-2009.
- Arras, C.; Wickert, J. Estimation of ionospheric sporadic E intensities from GPS radio occultation. *J. Atmos. Sol. Terr. Phys.* 2018, 171, 60–63, doi:10.1016/j.jastp.2017.08.006.
- Cai, H.; Li, F.; Shen, G.; Zhan, W.; Zhou, K.; McCrea, I.W.; Ma, S. E layer dominated ionosphere observed by EISCAT/ESR radars during solar minimum. *Ann. Geophys.* 2014, 32, 1223–1231, doi:10.5194/angeo-32-1223-2014.
- Mannucci, A.J.; Tsurutani, B.T.; Verkhoglyadova, O.; Komjathy, A.; Pi, X. Use of radio occultation to probe the high-latitude ionosphere. *Atmos. Meas. Tech.* 2015, 8, 2789–2800, doi:10.5194/amt-8-2789-2015.
- Reigber, C.; Lühr, H.; Schwintzer, P. CHAMP mission status. *Adv. Space Res.* 2002, 30, 129–134, doi:10.1016/S0273-1177(02)00276-4.
- Reigber, C.; Lühr, H.; Schwintzer, P.; Wickert, J. Earth Observation with CHAMP: Results from Three Years in Orbit; Springer: Berlin, Germany, 2005; ISBN 978-3-540-26800-0.
- Rocken, C.; Kuo, Y.H.; Schreiner, W.S.; Hunt, D.; Sokolovskiy, S.V.; McCormick, C. COSMIC System Description. *Terr. Atmos. Ocean. Sci.* 2000, 11, 21–52, doi:10.3319/tao.2000.11.1.21(cosmic).
- Liou, Y.A.; Pavelyev, A.G.; Liu, S.F.; Pavelyev, A.A.; Yen, N.; Huang, C.Y.; Fong, C.J. FORMOSAT-3/COSMIC GPS Radio Occultation Mission: Preliminary Results. *IEEE Trans. Geosci. Remote Sens.* 2007, 45, 3813–3826, doi:10.1109/TGRS.2007.903365.
- Anthes, R.A.; Bernhardt, P.A.; Chen, Y.; Cucurull, L.; Dymond, K.F.; Ector, S.; Healy, S.B.; Ho, S.P.; Hunt, D.C.; Kuo, Y.H.; et al. The COSMIC/FORMOSAT-3 mission: Early results. *Bull. Am. Meteorol. Soc.* 2008, 89, 313–333, doi:10.1175/BAMS-89-3-313.



References

- Fong, C.J.; Whiteley, D.; Yang, E.; Cook, K.; Chu, V.; Schreiner, B.; Ector, D.; Wilczynski, P.; Liu, T.Y.; Yen, N. Space and ground segment performance and lessons learned of the FORMOSAT-3/COSMIC mission: Four years in orbit. *Atmos. Meas. Tech.* 2011, 4, 1115–1132, doi:10.5194/amt-4-1115-2011.
- Yue, X.; Schreiner, W.S.; Lei, J.; Sokolovskiy, S.V.; Rocken, C.; Hunt, D.C.; Kuo, Y.H. Error analysis of Abel retrieved electron density profiles from radio occultation measurements. *Ann. Geophys.* 2010, 28, 217–222, doi:10.5194/angeo-28-217-2010.
- Davies, K. *Ionospheric Radio*; The Institution of Engineering and Technology: London, UK, 1990; ISBN 978-0863411861.
- Magnetic North, Geomagnetic and Magnetic Poles-WDC Kyoto. Available online: <http://wdc.kugi.kyoto-u.ac.jp/poles/polesexp.html> (accessed on 26 November 2019).
- Doherty, P.H.; Klobuchar, J.A.; Kunches, J.M. Eye on the Ionosphere: The Correlation between Solar 10.7 cm Radio Flux and Ionospheric Range Delay. *GPS Solut.* 2000, 3, 75–79, doi:10.1007/PL00012820.
- Jayachandran, P.T.; Donovan, E.F.; MacDougall, J.W.; Moorcroft, D.R.; Liou, K.; Newell, P.T.; St-Maurice J.P. Global and local equatorward expansion of the ion auroral oval before substorm onsets. *J. Geophys. Res.* 2005, 110, doi:10.1029/2004JA010837.
- Bai, W.H.; Sun, Y.Q.; Du, Q.F.; Yang, G.L.; Yang, Z.D.; Zhang, P.; Bi, Y.M.; Wang, X.Y.; Cheng, C.; Han, Y. An introduction to the FY3 GNOS instrument and mountain-top tests. *Atmos. Meas. Tech.* 2014, 7, 1817–1823, doi:10.5194/amt-7-1817-2014.
- Mao, T.; Sun, L.; Yang, G.; Yue, X.; Yu, T.; Huang, C.; Zeng, Z.; Wang, Y.; Wang, J. First Ionospheric Radio-Occultation Measurements From GNSS Occultation Sounder on the Chinese Feng-Yun 3C Satellite. *IEEE Trans. Geosci. Remote Sens.* 2016, 54, 5044–5053, doi:10.1109/TGRS.2016.2546978.
- Sun, Y.; Bai, W.; Liu, C.; Liu, Y.; Du, Q.; Wang, X.; Yang, G.; Liao, M.; Yang, Z.; Zhang, X.; et al. The FengYun-3C radio occultation sounder GNOS: A review of the mission and its early results and science applications. *Atmos. Meas. Tech.* 2018, 11, 5797–5811, doi:10.5194/amt-11-5797-2018.